European Commission

JRC TECHNICAL REPORTS

Characterisation of c-Si modules after 20 years of outdoor exposure on an electric vehicle.

Juan Lopez-Garcia
Tony Sample

2017

Joint Research Centre

EUR 28529 EN

This publication is a Technical report by the Joint Research Centre (JRC), the European Commission's science and knowledge service. It aims to provide evidence-based scientific support to the European policymaking process. The scientific output expressed does not imply a policy position of the European Commission. Neither the European Commission nor any person acting on behalf of the Commission is responsible for the use that might be made of this publication.

Contact information

Dr. Juan Lopez-Garcia
Address: Joint Research Centre, Via Enrico Fermi 2749, TP 450, 21027 Ispra (Va) Italy
Email: juan.lopez-garcia@ec.europa.eu
Tel.: +39 0332 78 3720

JRC Science Hub

https://ec.europa.eu/jrc

JRC105908

EUR 28529 EN

PDF	ISBN 978-92-79-66938-5	ISSN 1831-9424	doi:10.2760/38144
Print	ISBN 978-92-79-66937-8	ISSN 1018-5593	doi:10.2760/658440

Luxembourg: Publications Office of the European Union, 2017

How to cite this report: Lopez Garcia J; Sample T. *Characterisation of c-Si modules after 20 years of outdoor exposure on an electric vehicle.* EUR 28529 EN. Luxembourg (Luxembourg): Publications Office of the European Union; 2017. JRC105908 DOI:10.2760/38144

Contents

ABSTRACT

Characterisation of 4 crystalline silicon photovoltaic modules mounted on an electric vehicle and exposed outdoor for more than 20 years was performed. Heavy soiling was apparent and manual cleaning led to an average increase of Pmax of 14%, due mainly to an increase in Isc. One of the modules presented a severe damage with a FF below 37% and a decrease in the Pmax around -55%. An annual degradation rate of -0.24% for the module on the bonnet (different manufacturer than the other modules) and between -0.84 to -2.75% for the other modules was obtained, being slight greater than other reported values for crystalline silicon bared modules. The visual inspection showed modules heavily soiled and different defects, such as finger interruptions, discoloration, delamination and broken cells were apparent. Electroluminescence and IR imaging enabled the identification of modules with defects of the cells that can cause high cell temperatures during module operation, potentially leading to damages and a relation between the soiling parts and the relative EL intensity was found.

1 INTRODUCTION

The study of degradation of photovoltaic (PV) modules that have been field exposed for long periods of time is fundamental for identifying failure modes that have a direct influence in the photovoltaic module lifetime. These should be then replicated by appropriately designed accelerated stress tests, which would enable the designing of test protocols for ensuring higher PV module reliability. The effort to assure reliability of PV modules has resulted in the introduction by the International Electrochemical Commission (IEC) of accelerated test procedures (Design Qualification and Type Approval tests) IEC 61215 for terrestrial crystalline Si-based PV modules [1], that help manufactures to assess module reliability. However, the complex interaction of multiple stresses which takes place during long-term outdoor field exposure cannot be, or are difficult, to simulate under laboratory conditions during time constrained accelerated test. The module components are exposed to several factors such as solar radiation and its UV component, the heating effect of the solar radiation, weathering effects (rainfall, snow, wind, etc), the presence of dust and shadowing effects [2]. Therefore, the experimental studies on long-term outdoor exposure are of high importance and many studies which have been reported up to now, have been summarized in a review paper on degradation [3]. There are a great number of publications reporting on long-term degradation close too or in the range of the warranty period of 20-25 years [2, 4-12].

This work reports on the characterization of crystalline silicon modules mounted on an electric car and outdoor exposed for a period of around 20 years without cleaning in a moderate subtropical climate. Besides electrical performance measurements the modules were characterized using visual inspection, electroluminescence and thermal imaging. Typically, the PV module degradation analyses are carried out with modules mounted in an open rack configuration with a tilt angle of 30-45 degrees. In this work, a different environment with variable conditions (complete or partial shading, non-continuous use of battery or the chargers, near horizontal module mounting, vibrations, etc) for the module degradation is analysed.

2 EXPERIMENTAL METHOD

2.1 Modules characteristics

The modules used for this study consists of crystalline silicon modules that were manufactured in the mid-1980's. However, they were installed in the solar vehicle in the mid-1990's. 3 modules were installed on the roof (ESTI codes IY42, IY43, IY44) and 1 (ESTI code IY41) on the bonnet of a small car, while 2 modules of the same type as IY42, IY43 and IY44 were stored indoors to be used as reference samples (IY45 and IY46). Two different types of modules were used which differed in the manufacturer and in the number of cells (36 in one module and 33 in the others). Each module had 10x10 cm size monocrystalline silicon solar cells connected in series (Table I).

Figure 1 View of the photovoltaic modules on the electric vehicle.

The IY41 module was mounted in the bonnet of the car with a tilt angle of 12 degrees. The IY42 and IY44 were mounted on the roof of the car with a tilt angle of 8 degrees meanwhile the IY43 remained horizontal on the roof, subjected to long-term continuous outdoor exposure for more than 20 years without cleaning (Figure 1 and Figure 2). The car was a Mazzieri model with an electric motor of 7 cV of maximum power and a maximum speed of 70 Km/h. The average energy consumption is 20 kWh/100 Km according to ECE test cycle and the minimum range is 100Km by road, at 80% depth of discharge (DOD). The modules were connected to a battery and the electric vehicle was used as service car within the JRC and for occasional journeys to regions near Ispra.

The climatic conditions of Ispra (located in northern Italy) at 220 m above sea level, where the weathering took place, are considered to be a moderate subtropical climate (-10°C to +35 °C, with less than 90% RH).

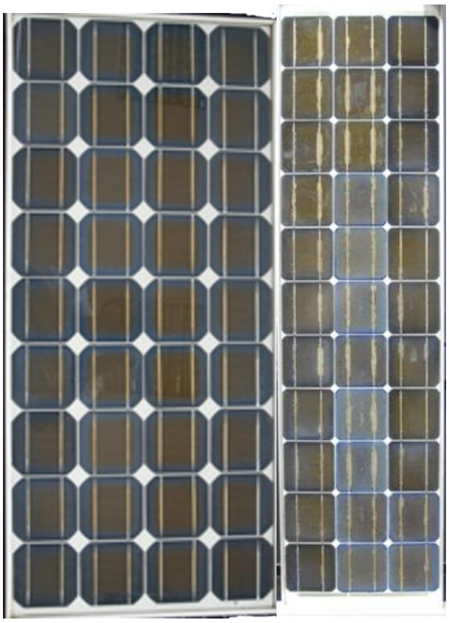

Figure 2 Module type 1 (BP) and module type 2 (Arcosolar) after 20 years of outdoor exposure on the electric car.

Table I Module characteristics.

Code	Manufacturer	Model	Front glass	Encapsulant	N. of cells	Bypass diode	Cell size (cm)	Years outdoor	Cell layout
IY41	BP	1242	Flat	EVA	36	Yes	10x10	20	1 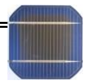
IY42	Arcosolar	M75	Flat	EVA	33	Yes	"	20	2
IY43	Arcosolar	"	Flat	EVA	33	Yes	"	20	2 
IY44	Arcosolar	"	Flat	EVA	33	Yes	"	20	2
IY45	Arcosolar	"	Flat	EVA	33	Yes	"	Not exposed	2

2.2 Characterization methods

Before being installed in the vehicle, IY41 was characterised by I-V measurements at ≈1000W/m^2 and 25°C and it was subjected to several tests according to protocol CEC501 [13] and CEC502 [14], early versions of type approval tests, which included visual inspection, insulation test, thermal cycling, humidity freeze, hot spot testing, etc. The spectral responsivity was not measured, therefore the mismatch factor could not be calculated and the IV curve was not corrected to STC. Since initial measurements are not available for the other modules, the rated values observed in the label were taken as initial values. It should be noted that the modules were manufacture in the mid to late 1980's and mounted on the electric car in the mid-1990. Since no additional information has been found, it has been considered that the modules were stored indoors and the PV module degradation was negligible until they were mounted on the car.

After removing the modules from the vehicle, a series of characterizations were performed on all modules, including:

- Detailed visual inspection
- I-V curve measurements with a flash tester at ≈1000W/m^2 and 25°C, with all measurements corrected to 1000W/m^2.
- Electroluminescence
- Thermal imaging for hot spot detection

The modules were not cleaned during the outdoor exposure period; therefore long-term soiling accumulated on the surface and edges and was removed by using a soft sponge with a standard commercially available glass cleaning detergent sprayed on the cover glass and a final clean with a cloth. Times of approximately 10 minutes were employed for each module during the manual cleaning.

2.2.1 Detailed visual inspection

The detailed visual inspection followed the procedure proposed in [15] which is based on a quantitative classification of defects. The approach is a quantitative one, with the collection not only of the defects types, but also of their occurrence and area covered by them. This differs from the approach of IEC 61215, where the defects are categorized as "minor" if they are allowed for type approval or “major” in case of defects not acceptable for type approval, but without the requiring the quantification of defects in most of the cases.

2.2.2 I-V measurement set-up

In 2015, I-V curves were measured using the Pasan IIIB flash simulator, having a flash duration of 10ms. This system presents some differences compared to the one used to characterize the IY41 module in 1988, which had a shorter flash duration with an I-V curve sweep of 1.5ms. Also the reference cells used for the measurements in 1988 and in 2015 were different. It has been previously reported the potential difference introduced in the measurements by the setup used in the 1980's and the one used in 2015 at the ESTI laboratory [16]. Since there are no initial measurements available of the stored modules IY45, IY46 nor a reference module similar to IY41, the results of the cited work with similar crystalline silicon modules manufacturer in the same date are extrapolated. It was observed that part of the differences in measurements found using the two setups can be attributed to the enhanced temperature control that was implemented between the 1980's and 2015 and to the different spectrum of the two simulators. Another factor that had an influence was the different reference cell used to measure the modules in 1980's and in 2015. Given these differences, the measurements performed in 1980's and in 2015 were found to be of similar order, therefore giving confidence that the changes measured after long-term exposures are the result of ageing.

2.2.3 Electroluminescence and thermal imaging

Electroluminescence (EL) images were performed in darkness with the module forward biased at I_{sc} with an exposure of 300 seconds using a Sensovation digital camera SVSB14-M. Data were analysed with a free software "dataArtist" developed by CREST at University of Loughborough.

Infrared thermography images were performed with a Fluke Ti55 camera under two conditions:

- With the module forward biased to current equivalent to I_{sc} (Bias).
- Under continuous exposure to light (≈1000 W/m^2) provided by a steady state solar simulator and short circuited with a 15Ω resistance (illuminated).

In both cases, the modules were mounted in a fixed vertical rack.

3 RESULTS AND DISCUSSION

3.1 Detailed visual inspection

After removal from the electric car, visual inspection was performed on all modules, and some defects were categorised according to the visual inspection data collection tool. Soiling was present in all modules, due to the fact that no cleaning was performed after installation on the car. As the modules were mounted with a low tilt angle or almost horizontal configuration, the soiling was uniformly distributed across the module. In the case of the modules with a minor inclination, soiling was more pronounced in the lower part of the module, close to the frame where soiling accumulated more easily (Figure 3).

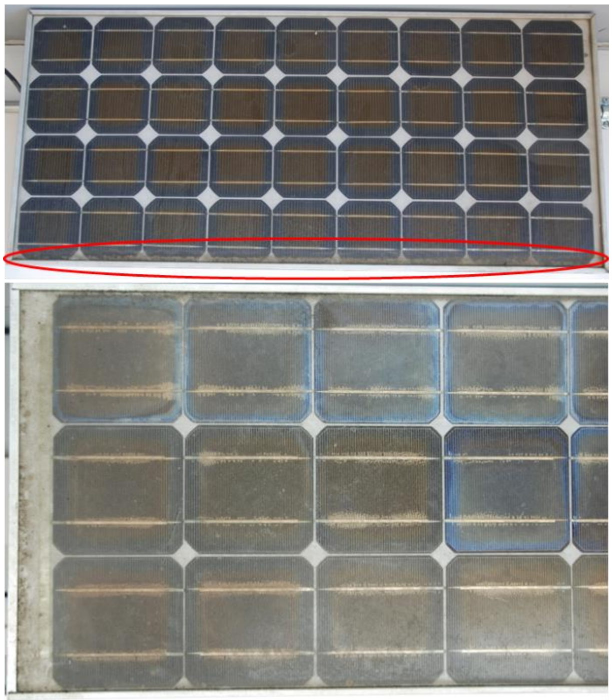

Figure 3 soiling accumulating at the lower edge of a module near the frame and uniformly on the glass.

As already reported in previous works [4, 17] some defects are related to the properties of the materials used for manufacturing the modules and therefore affect all modules. Examples of these defects are minor backsheet discoloration, due to properties of the tedlar used as backsheet (as the modules are mounted in direct contact to the roof or the bonnet of the car with low tilt angle, not relevant damages were observed in the backsheet and in the junction box) and discoloration of cell's fingers, due to degradation of the metallization grid. Examples of the usual defects found in some of the modules are shown in Figure 4. They include different types of delamination of the encapsulant close to the cell interconnect ribbons and over the cell, respectively (Figure 4a and 4d), cracked cell, degradation and discoloration of cell interconnect ribbons and busbars, discoloration or yellowing over center of the cells and discoloration over whole cell.

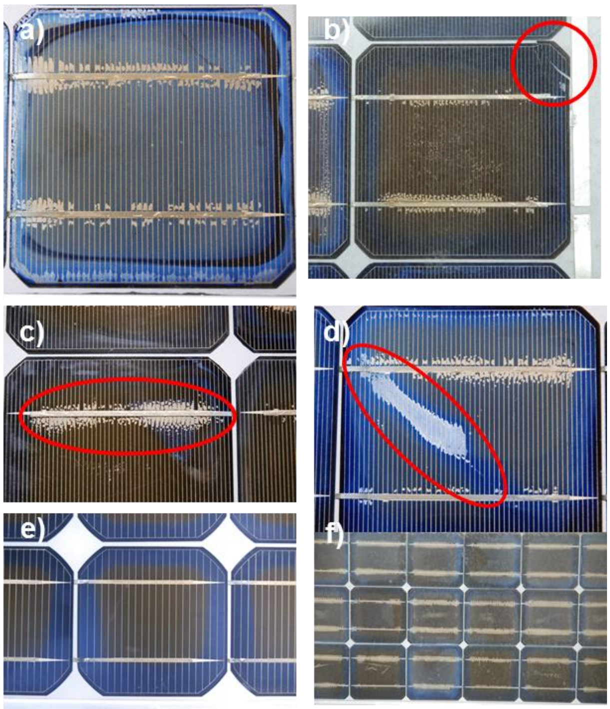

Figure 4 Examples of visual defects: different types of delamination (close to the cell interconnect ribbons and over the cell, respectively) (a),(d), cracked cell (b), degradation and discoloration of cell interconnect ribbons and busbars (c), discoloration or yellowing over center of the cells (e) and discoloration over whole cell (f).

3.2 Electrical performance

Figure 5 shows the I-V curves of different modules of the same type before and after a manual cleaning after 20 years of outdoor exposure on an electric vehicle and a reference module stored indoor in the basement. The kink in the I-V curves of soiled modules can be observed, and this suggests non-uniform shading. However, the kink in the modules IY42 and IY44 do not disappear after the manual cleaning that suggest other factors, for example, mismatch between cells, damaged or cracked cells. On the other hand, the I_{sc} of the module IY43 is increased after manual cleaning but this module presents a severe failure and the FF decrease below 38%. Table II presents the change (in %) of the electrical parameters of the modules mounted in the car before and after manual cleaning expressed as:

$$P_{max} change\ (\%) = \frac{P_{\max\ after\ cleaning} - P_{\max\ soiled}}{P_{\max\ soiled}} \times 100 \quad (1)$$

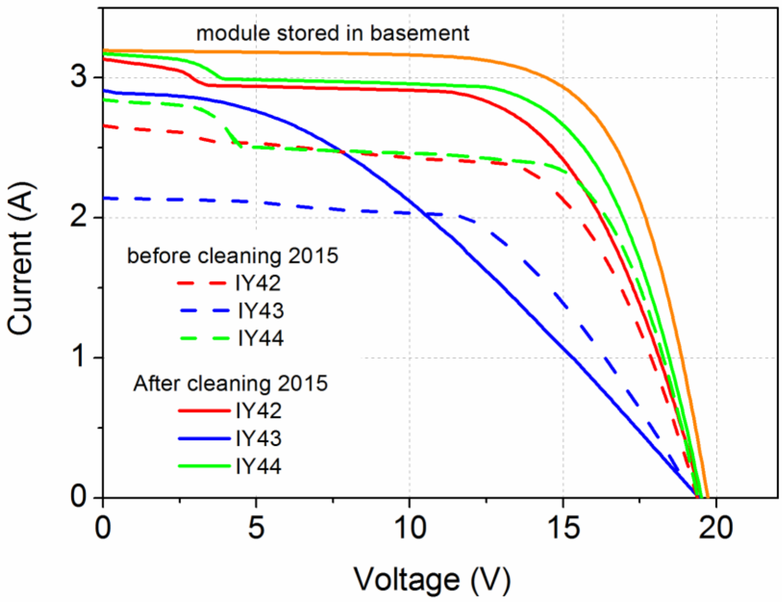

Figure 5 I-V curves of different modules of the same type before cleaning and after manual cleaning after 20 years of outdoor exposure on an electric car.

Where $P_{max\ soiled}$ is the P_{max} (or other electrical parameter) of the soiled module before cleaning manually. It is clearly observed that the increase in the P_{max} of the modules (except in the module IY43) is due to an increase in the I_{sc} and in the I_{mpp}. This improvement in the P_{max} after cleaning is significantly greater than other reported values for long-term soiling around 9.8% [18]. P_{max} decrease significantly after manual cleaning for IY43 due to a marked decrease of the FF (-34.1%) that means that severe failure modes were presented in the module and covered by the soiling. This indicates that flat mounting has an impact on soiling.

Figure 6 shows the I-V curves of the module IY41 measured initially in 1988 and measured in 2015 before and after manual cleaning. It is also observed the kink in the I-V curve due to the soiling.

Table II change (%) of the electrical parameters of the whole set of modules exposed before cleaning and after manual cleaning after 20 years of outdoor exposure on an electric car.

Module Code	Δ I_{sc} (%)	Δ V_{oc} (%)	Δ P_{max} (%)	Δ FF (%)	Δ I_{mpp} (%)	Δ V_{mpp} (%)
IY41	**10.20**	0.63	**14.98**	3.69	17.16	-1.86
IY42	**17.95**	0.70	**13.77**	-4.21	15.05	-1.11
IY43	**36.01**	0.75	**-9.70**	-34.10	5.99	-14.81
IY44	**11.06**	0.58	**13.63**	1.71	16.79	-2.71

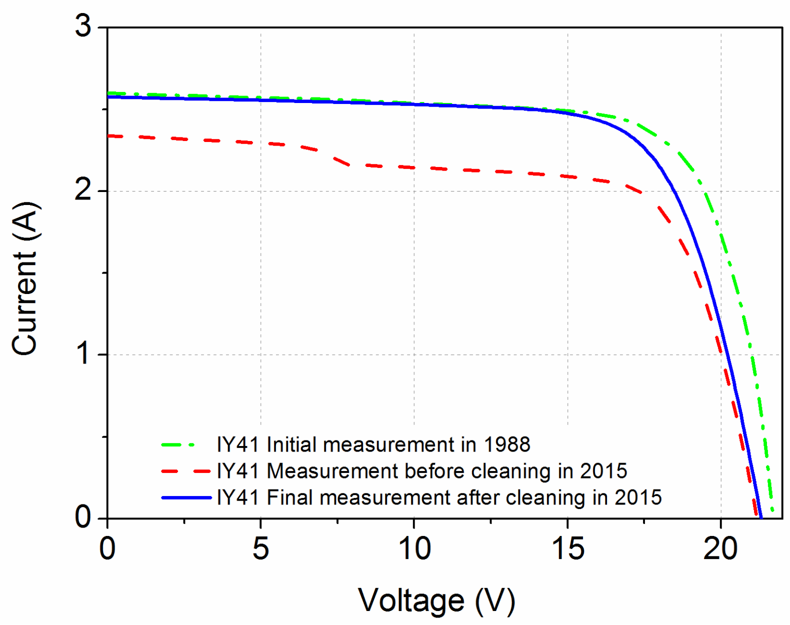

Figure 6 I-V curves of the module IY41 after more than 20 years of outdoor use on an electric car.

The impact of soiling can be reversible as after a cleaning procedure, soiling was no longer evident. Several studies have quantified the effects of soiling on electrical performances of modules [19, 20].

The changes in the electrical parameters after long-term exposure (20 years) on the electric car are presented in the table III. As mentioned in the previous section, there are no initial measurements available for modules IY42, IY43, IY44 and the rated values have been taken as initial reference measurements. The module IY41 exhibited a small P_{max} decay (-4.69%) in comparison to the other modules mainly due to a decay in the V_{oc}. However, the P_{max} decay (between -16% and -55% for the damage module, IY43) for the other modules is extremely high and due to a decay in the I_{sc} and V_{oc}. It has been reported that the average difference between the rated values and the measurement (at ESTI) P_{max} in the 1980's was around -4.5% [21]. It was also published by Reis *et al.* that the module type under study (referring to IY42-IY44) showed a field performance 8.9% below their nameplate ratings[22]. This means that even with these differences, the P_{max} decay remain between -13% (-8.7%) and -53% (-51%). These values imply an average annual degradation rate ranged between -0.84 to -2.75 for the modules IY42-IY44 and around -0.24% per year for the IY41. In general, it has been reported that the degradation rates distribution exhibits on average a -0.5% to -1% P_{max} decay per year.

Table III change (%) of electrical parameters from rated values* or measured in the 1988** and measured 2015.

Module Code	Δ I_{sc} (%)	Δ V_{oc} (%)	Δ FF(%)	Δ P_{max} (%)
IY41**	-0.90	-1.79	-1.96	**-4.69**
IY42*	-10.18	-11.30	-3.38	**-23.02**
IY43*	-16.61	-11.70	-39.24	**-55.26**
IY44*	-16.14	-11.31	11.71	**-16.91**

We have also compared the measurements after cleaning in 2015 some modules (IY42, IY43 and IY44) with the values of a reference module of the same type stored indoor in the basement for the same period of time (IY45) also measured in 2015. The results are shown in Table IV. This comparison indicates the electrical parameter values if the modules were not used on the electric car. It is clearly observed that the module IY43 is damaged and the P_{max} decay is around -50.13%. The other two modules exhibit P_{max} decay of -14.20% and -9.60% which correspond to annual degradation rate of -0.7% and -0.5%, respectively, in agreement with the reported values for crystalline silicon PV modules installed in an open rack. From the table III and Table IV (rated values and measured value sin 2015), we can estimate the degradation in P_{max} for the reference module stored in the basement lower than -10% over more than 27 years from the date of fabrication that it is within the tolerance range.

Table IV change (%) of electrical parameters from the module stored in the basement (IY45) and the modules (IY42, IY43 and IY44) after manual cleaning measured both in 2015.

Module Code	Δ I_{sc} (%)	Δ V_{oc} (%)	Δ P_{max} (%)	Δ FF (%)	Δ I_{mpp} (%)	Δ V_{mpp} (%)
IY42	-2.95	-0.56	**-14.20**	-11.10	-7.85	-6.89
IY43	-9.89	-1.01	**-50.13**	-44.09	-29.26	-29.50
IY44	-2.99	-0.55	**-9.60**	-6.29	-5.84	-3.99

3.3 Electroluminescence and thermography analysis

Electroluminescence (EL) images of modules mounted on the electric car and the corresponding IR thermography images obtained on the module subjected to continuous illumination, with an appropriate resistive load connected, and on the module biased at

I_{sc} are shown in figure 7 for IY41 and in figure 8a, b, c and d for modules IY42, IY43, IY44 and the reference module IY45. Since the measurement conditions were the same in all cases (same exposure time, same distance between module and camera, etc), the intensity of the EL signal can be related to the module performance as it is related to the minority carrier diffusion length [23]. It is also shown in figure 7 and 8 the relative EL intensity (100 for the most intense and 0 for the least intense cell) of each cell (yellow square for cells with less than 50% of the maximum EL intensity and red fill square for cells greater than 50% of the least intense cell). Partially inactive areas and a significant number of grid finger interruptions have been detected in all modules by the EL images.

0	95	79	60	76	60	**100**	98	91
87	91	57	78	43	2	62	66	1
81	80	81	86	82	75	49	30	28
27	33	35	32	30	48	59	45	46

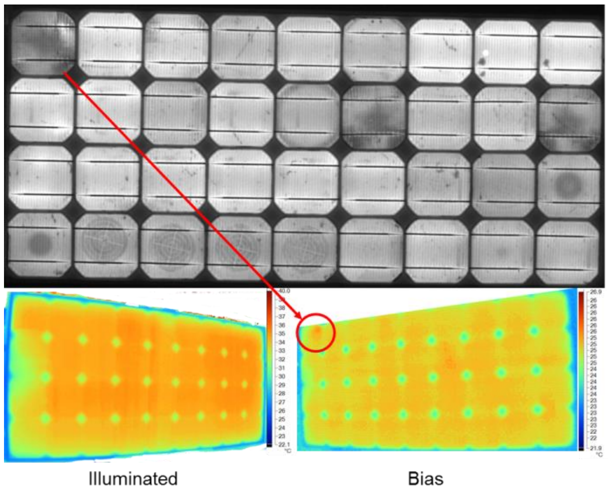

Figure 7 EL images of IY41, relative EL intensity and the respective IR thermography images using continuous light exposure (left) and forward biased module (right).

IY41 presents a homogeneous temperature distribution with only one point hotter than the rest corresponding to the cell with the lower EL intensity. The EL image shows darker cells (with EL intensity below 50%) corresponding to the cells in bottom part of the module close to the edge heavily soiled. However, severely damaged cells were not observed in the EL image (figure 7) for module IY41 in agreement with the I-V measurements. Figure 8a also shows EL intensities below 50% of the maximum on the heavily soiled edge of the module IY42 (top line of the EL intensity table). A spot of significant higher temperature are observed in two cells by IR thermography when a bias is applied corresponding to focalized regions of higher resistance along the cell interconnect ribbons. The EL and IR image of the damage module IY43 is shown in figure 8b. EL image exhibits brighter spots localized along and close to the busbar or cell interconnect ribbons with a higher resistance that leads to spots of higher temperature as observed in the IR thermography image. The cell with the lowest EL intensity presents a crack between the busbar but it is not reflected as a hot spot. Figure 8c and 8d show the EL images and IR thermography of the modules IY44 and IY45, respectively. No appreciable damage or hot spots are observed and more than 70-75 % of the cells present a relative EL intensity greater than the 50% of the minimum value. EL image of IY44 (Figure 8c) shows the inactive area of the broken cell (first column, second row) and a relative high number of finger interruptions.

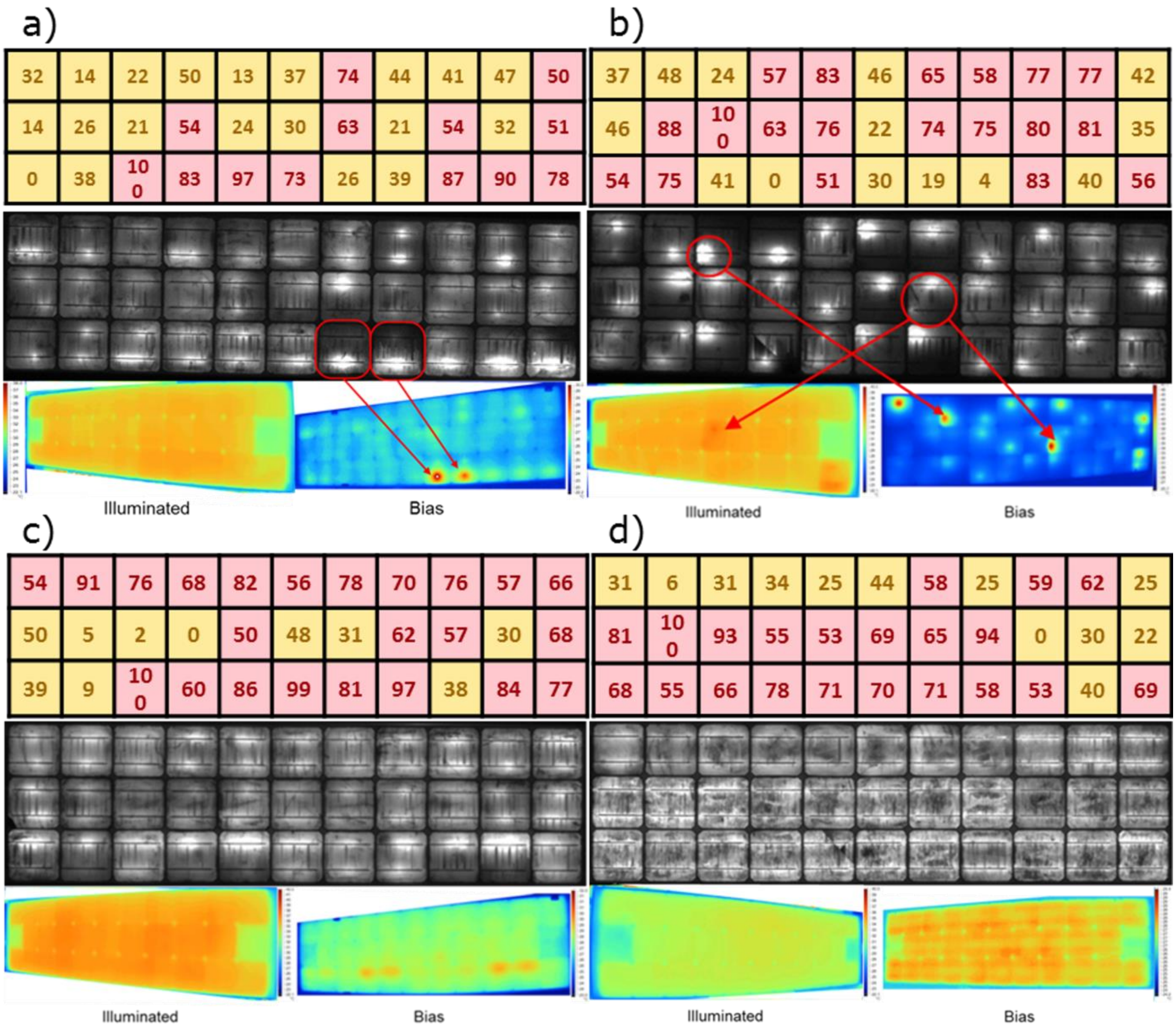

Figure 8 EL images, relative EL intensity and the respective IR thermography images using continuous light exposure (left) and forward biased module (right), of the IY42 (a), IY43 (b), IY44 (c) and the module stored in the basement IY45 (d).

The ranking of the absolute average EL intensity of the modules (IY42, IY43, IY44 and IY45 reference module) agree with the order of the modules organized by their P_{max} after manual cleaning.

4 CONCLUSIONS

Characterisation of 4 crystalline silicon photovoltaic modules mounted on an electric vehicle and exposed outdoor for more than 20 years was performed. Heavy soiling was apparent and manual cleaning led to an average increase of P_{max} of 14%, due mainly to an increase in I_{sc}. One of the modules presented a severe damage with a FF below 37% and a decrease in the P_{max} around -55%. An annual degradation rate of -0.24% for the module on the bonnet (different manufacturer than the other modules) and between -0.84 to -2.75% for the other modules was obtained, being slight greater than other reported values for crystalline silicon bared modules.

The visual inspection showed modules heavily soiled and different defects, such as finger interruptions, discoloration, delamination and broken cells were apparent.

Electroluminescence and IR imaging enabled the identification of modules with defects of the cells that can cause high cell temperatures during module operation, potentially leading to damages and a relation between the soiling parts and the relative EL intensity was found.

5 REFERENCES

[1] International Electrotechnical Commission, IEC 61215 ed 2.0 Crystalline silicon terrestrial photovoltaic (PV) modules: design qualification and type approval, IEC, 2005.

[2] C.R. Osterwald, A. Anderberg, S. Rummel, L. Ottoson, Degradation analysis of weathered crystalline-silicon PV modules, in: Photovoltaic Specialists Conference, 29th IEEE Photovoltaic Specialist Conference, 2002, pp. 1392-1395.

[3] D.C. Jordan, S.R. Kurtz, Photovoltaic degradation rates - An Analytical Review, Prog Photovoltaics Res Appl, 21 (2013) 12-29.

[4] D. Polverini, M. Field, E. Dunlop, W. Zaaiman, Polycrystalline silicon PV modules performance and degradation over 20 years, Prog Photovoltaics Res Appl, 21 (2013) 1004-1015.

[5] E.D. Dunlop, Lifetime performance of crystalline silicon PV modules, 3rd World Conference on Photovoltaic Energy Conversion, 2003, pp. 2927-2930.

[6] E.D. Dunlop, D. Halton, The performance of crystalline silicon photovoltaic solar modules after 22 years of continuous outdoor exposure, Prog Photovoltaics Res Appl, 14 (2006) 53-64.

[7] E.D. Dunlop, D. Halton, H.A. Ossenbrink, 20 years of life and more: Where is the end of life of a PV module?, 31st IEEE Photovoltaic Specialists Conference, 2005, Lake Buena Vista, FL, 2005, pp. 1593-1596.

[8] D.C. Jordan, B. Sekulic, B. Marion, S.R. Kurtz, Performance and Aging of a 20-Year-Old Silicon PV System, IEEE J. Photovoltaics, 5 (2015) 744-751.

[9] M.A. Quintana, D.L. King, T.J. McMahon, C.R. Osterwald, Commonly observed degradation in field-aged photovoltaic modules, 29th IEEE Photovoltaic Specialists Conference, New Orleans, LA, 2002, pp. 1436-1439.

[10] A. Skoczek, T. Sample, E.D. Dunlop, The results of performance measurements of field-aged crystalline silicon photovoltaic modules, Prog Photovoltaics Res Appl, 17 (2009) 227-240.

[11] A. Realini, E. Bura, N. Cereghetti, D. Chianese, S. Rezzonico, T. sample, H. Ossenbrink, Study of a 20 year old PV plant (MTBF project), 17th European PV Solar Energy Conference, Munich, Germany, 2001, pp. 447-450.

[12] E. Lorenzo, R. Zilles, R. Moretón, T. Gómez, A. Martínez De Olcoz, Performance analysis of a 7-kW crystalline silicon generator after 17 years of operation in Madrid, Prog Photovoltaics Res Appl, 22 (2014) 1273-1279.

[13] European Commission, Qualification Test Procedures for Photovoltaic Modules: CEC-Specifications No. 501, EUR Report 7545 EN, in, 1981.

[14] European Commission, Qualification Test Procedures for Photovoltaic Modules: CEC-Specification No. 502 (Issue 1), in, 1984.

[15] C.E. Packard, J.H. Wohlgemuth, S.R. Kurtz, Development of a Visual Inspection Data Collection Tool for Evaluation of Fielded PV Module Condition, Technical Report NREL/TP-5200-56154 NREL, Golden, Colorado, 2012.

[16] J. Lopez-Garcia, A. Pozza, T. Sample, Analysis of crystalline silicon PV modules after 30 years of outdoor exposure, 31th European Photovoltaic Solar Energy Conference and Exhibition, Hamburg, Germany, 2015, pp. 1847 - 1853.

[17] A. Pozza, T. Sample, Electrical Analysis and Characterization by LBIC and Electroluminescence of Crystalline Silicon PV Modules After Approximately 20 Years of Field Exposure, 29th European Photovoltaic Solar Energy Conference and Exhibition, Amsterdam, Netherlands, 2014, pp. 2523 - 2529.

[18] J. Lopez-Garcia, A. Pozza, T. Sample, Long-term soiling of silicon PV modules in a moderate subtropical climate, Sol. Energy, 130 (2016) 174-183.

[19] C. Schill, S. Brachmann, M. Heck, K.A. Weiss, M. Koehl, Impact of heavy soiling on the power output of PV-modules, Proc SPIE Int Soc Opt Eng, 8112 (2011).

[20] C. Schill, S. Brachmann, M. Koehl, Impact of soiling on IV-curves and efficiency of PV-modules, Sol. Energy, 112 (2015) 259-262.

[21] J. Lopez-Garcia, T. Sample, Evolution of measured module characteristics versus labelled module characteristics of crystalline silicon based PV modules., to be summited to Solar Energy, (2016).

[22] A.M. Reis, N.T. Coleman, M.W. Marshall, P.A. Lehman, C.E. Chamberlin, Comparison of PV module performance before and after 11-years of field exposure, 29th IEEE Photovoltaic Specialists Conference, New Orleans, LA, 2002, pp. 1432-1435.

[23] T. Fuyuki, H. Kondo, Y. Kaji, A. Ogane, Y. Takahashi, Analytic findings in the electroluminescence characterization of crystalline silicon solar cells, J Appl Phys, 101 (2007).

Acknowledgements

The authors would like to thank to Pierangelo Biavaschi and Franseco Noseda for the help with the dismantling of the PV modules.

Authors

Lopez-Garcia, Juan and Sample, Tony

KJ-NA-28529-EN-N

JRC Mission

As the science and knowledge service of the European Commission, the Joint Research Centre's mission is to support EU policies with independent evidence throughout the whole policy cycle.

EU Science Hub
ec.europa.eu/jrc

@EU_ScienceHub

EU Science Hub - Joint Research Centre

Joint Research Centre

EU Science Hub

Publications Office

doi:10.2760/38144

ISBN 978-92-79-66938-5